Extended Abstracts of the 2012 International Conference on Solid State Devices and Materials, Kyoto, 2012, pp753-754

Comparative Study of Schottky Barrier Height Modulation in S-introduced NiGe/Ge and NiSi/Si Junctions

Masahiro Koike, Yuuichi Kamimuta, and Tsutomu Tezuka
Green Nanoelectronics Center (GNC), National Institute of Advanced Industrial Science and Technology (AIST)
West 7A, Onokawa 16-1, Tsukuba, Ibaraki, 305-8569, Japan
Phone: +81-29-849-1081 Fax: +81-29-849-1186 massahiro.koike@aist.go.jp

I. Introduction

The segregation of impurities around the NiGe/Ge interface has received considerable attention as a means of modulating the contact resistance of NiGe/*n*Ge junctions for Ge *n*MOSFETs with high I_{ON} and low I_{OFF}. For P-segregated NiGe/Ge, ohmic characteristics of *n*Ge and rectifying characteristics of *p*Ge have been observed [1]. For S-segregated NiGe/*n*Ge, a low Schottky barrier height (SBH) of 0.15 eV was estimated using an Arrhenius plot [2]. We have investigated chalcogen (S, Se, or Te)- and/or P-introduced NiGe/Ge diodes [3]-[5], and found that their co-introduction was more effective in reducing the SBH for *n*Ge and increasing the SBH for *p*Ge; however, the dependence on the S dose has not been clarified. In S-segregated NiSi/*n*Si, on the other hand, lower SBH values of 0.07 eV [6] and 3.4 meV [7] have been reported. The introduction of S appears to reduce the SBH more for NSi/*n*Si than for NGe/*n*Ge. To our knowledge, however, NiSi/Si and NiGe/Ge fabricated by the same process have not been investigated for the purpose of comparison. In this study, therefore, we have fabricated S-implanted Si and Ge substrates and NiSi/Si and NiGe/Ge diodes under various conditions including S-dose dependence, and investigated them to clarify the difference between them.

II. Experiment

NiX/X (X=Ge, Si) diodes were fabricated as follows: 4-inch *n* (*p*)-type X(100) wafers with SiO_2 isolation were implanted with S ions (8×10^{11}-5×10^{14} cm^{-2}), P ions (1×10^{15} cm^{-2}), or both. The acceleration energies of P and S were both 10 keV so as to achieve the same projected range values. Ni films (~15 nm) were deposited on the substrates by sputtering. Then, RTA was performed for NiGe at 250-450ºC (NiSi at 350-550ºC) in N_2 for 1 min. Unreacted Ni on NiX was removed by HCl solution. Al layers were formed on the back sides of the diodes by thermal evaporation to reduce the back contact resistance. For comparison, NiX/X diodes without introduced impurities were also fabricated as references. Profiles of the impurity concentration (N) and carrier concentration (n) were examined by SIMS and using a spreading resistance probe (SRP), respectively. The positions of the NiX/X interfaces were defined by the NiX thickness. *J*-*V* characteristics at 223–413 K were measured for the NiX/X diodes. The SBH (φ) was estimated in two ways: by theoretical fitting to the equation for Schottky current [8] at 300 K,

$$J=A^*T^2\exp(-q\varphi/k_BT)[\exp(qV/k_BT)-1] \quad (1),$$

and from the temperature (T) dependence of J, i.e., $\varphi=-(k_B/q)\Delta\log[|J|/T^2]/\Delta(1/T)$.

III. Results and discussion

First, we examined the profiles in P- and/or S-implanted X before NiX formation (Fig. 1). The profiles of impurity concentrations in the S-implanted Si did not indicate S diffusion after annealing. On the other hand, the SRP profiles revealed the generation of electrons. S in X is known to behave as a double donor and form two different donor levels: level E_1 occupied by one electron and level E_2 occupied by two electrons [Fig. 2(a)]. The occupation probabilities (f_1 and f_2) were derived as follows [5]:

$$f_1=2\exp[-(E_1-\mu)/k_BT]/\Xi \quad (2),$$

$$f_2=\exp[-2(E_2-\mu)/k_BT]/\Xi \quad (3),$$

where $\Xi:=1+2\exp[-(E_1-\mu)/k_BT]+\exp[-2(E_2-\mu)/k_BT]$. On the basis of these equations, we calculated the relationship between inverse temperature and concentration [Fig. 2(b)], which revealed a high electrical activation ratio of $n/N_D\approx 2-f_1-2f_2\approx1$. This implies that the electron generation in S-implanted X is reasonable and that the low n is due not to the low activation ratio but to the low solid solubility. In S-implanted X, n increased with increasing T and increasing S dose [Figs. 3(a) and 3(b)].

Under the same annealing conditions as those used to obtain the above profiles, we fabricated NiX/X diodes. SIMS profiles of NiSi/Si show that S segregated around the interface and that its concentration increased with increasing S dose (Fig. 4). Next, we investigated the *J*-*V* characteristics of the diodes. The *J*-*V* characteristics showed ohmic behavior for NiSi/*n*Si [Fig. 5(a)] and rectifying behavior for NiSi/*p*Si [Fig. 5(b)]. Although the *J*-*V* characteristics similarly showed almost ohmic behavior for NiGe/*n*Ge (Fig. 6), they still showed almost ohmic characteristics for NiGe/*p*Ge (see Fig. 10 later).

Here we summarize the relationship between the NiX formation temperature and the SBH estimated by theoretical fitting [Figs. 7(a) and 7(b)]. The SBH tended to decrease more with increasing S dose than with increasing T. We consider that SBH and n are probably determined by the solid solubility around the NiX/X interface, because the solid solubility basically depends on not the impurity dose but the annealing temperature.

Figure 8 shows the relationship between the two SBH values estimated in two ways. The SBH estimated from the T dependence (Fig. 9) was lower than that obtained by theoretical fitting to Eq. (1). This indicates that the *J*-*V* characteristics cannot be explained by the mechanism of Schottky current [8]. Although the formation of a S-Ge dipole layer and a decrease in the interface trap density, which leads to the lowering of the true SBH, are possible models, they cannot satisfactorily explain our results. It has been proposed that S reduces the contact resistance of NiSi/*n*Si through a doping effect rather than reduces the SBH [10]. This mechanism may be possible if the solid solubility limit of S in X around the interface is more than that in the bulk of X. In addition, we consider that another mechanism also acts at the same time [4]. If S exists in Ge around the interface, the current may mainly flow through the donor level of S. The lower activation energy corresponding to the donor level than that of the true SBH can be estimated from the T dependence. This model as well as the doping model [10] can explain the difference between the two SBHs.

Note that the data for NiSi/*n*Si and NiGe/*n*Ge (Fig. 8) are distributed on a similar curve, indicating that their SBH similarly decreased with increasing S dose; however, the *J*-*V* characteristics of NiSi/*p*Si showed rectifying behavior, whereas those of NiGe/*p*Ge still showed almost ohmic behavior. These behaviors can be explained by the difference in the band-gap energy between Si (1.12 eV at 300 K [8]) and Ge (0.66 eV at 300 K [8]). The SBH for NiSi/*p*Si was estimated to be ~0.5 eV, whereas that for NiGe/*p*Ge was ~0.1 eV (Fig. 7). Since the introduction of S decreased the SBH by ~0.3 eV at least for NiSi/*n*Si and that by ~0.2 eV for NiGe/*n*Ge, the SBH for S-introduced NiSi/*p*Si was estimated to be ~0.8 eV at least, leading to significant current reduction [Fig. 5(b)], whereas that for S-introduced NiGe/*p*Ge was estimated to be ~0.3 eV, leading to almost ohmic behavior [Fig. 10(b)]. Therefore, for NiSi/Si, the introduction of S is sufficiently effective in modulating the SBH. On the other hand, for NiGe/Ge, the introduction of S did not significantly reduce J for the *p*-type diodes. Therefore, it will be necessary to employ other methods such as the co-introduction of S with P into NiGe/Ge [3]-[5]. *J*-*V* characteristics for the P and S co-introduced NiGe/Ge diodes showed ohmic behavior for *n*-type diodes and rectifying behavior for *p*-type diodes (Fig. 10), although neither the introduction of only S nor that of only P was sufficient to modulate the SBH for Ge. Thus, P and S co-introduction is an effective way of modulating the SBH of NiGe/Ge.

IV. Summary

We investigated S-implanted Si and Ge and S-introduced NiSi/Si and NiGe/Ge fabricated under various conditions to clarify the difference between Si and Ge. The introductions of S similarly reduced the SBH of NiSi/*n*Si and NiGe/*n*Ge. On the other hand, the *J*-*V* characteristics of NiSi/*p*Si showed rectifying behavior, whereas those of NiGe/*n*Ge still showed almost ohmic behavior. This is mainly due not to the difference in the effect of S on the SBH but to the difference in the band-gap energy between Si and Ge. For NiGe/Ge, it was revealed that P and S co-introduction is effective in modulating the SBH.

Acknowledgment

This research was supported by a grant from JSPS through the FIRST Program initiated by CSTP.

References

[1] T. Nishimura, K. Kita, and A. Toriumi, Appl. Phys. Express **1**, 051406 (2008).
[2] K. Ikeda, Y. Yamashita, N. Sugiyama, N. Taoka, and S. Takagi, Appl. Phys. Lett. **88**, 152115 (2006).
[3] M. Koike, Y. Kamimuta, and T. Tezuka, Appl. Phys. Express **4,** 021301 (2011).
[4] M. Koike, Y. Kamimuta, and T. Tezuka, Ext. Abstr. Int. Conf. Solid State Devices and Materials, 909 (Nagoya, Japan, 2011).
[5] M. Koike, Y. Kamimuta, and T. Tezuka, Int. Workshop Junction Technol. Ext. Abstr. 222 (Shanghai, China, 2012).
[6] Q. T. Zhao, U. Breuer, E. Rije, St. Lenk, and S. Mantl, Appl. Phys. Lett. **86**, 062108 (2005).
[7] Y. –C. Yang, Y. Nishi, and A. Kinoshita, MRS Proc. **2009**, 1155.
[8] S. M. Sze, *Physics of Semiconductor Devices, 2nd ed* (Wiley, New York, 1981).
[9] H. G. Grimmeiss, L. Montelius, and K. Larsson, Phys. Rev. B **37**, 6916 (1988).
[10] J. Chan, N. Y. Martinez, J. J. D. Fitzgerald, A. V. Walker, R. A. Chapman, D. Riley, A. Jain, C. L. Hinkle, and E. M. Vogel, Appl. Phys. Lett. **99**, 012114 (2011).

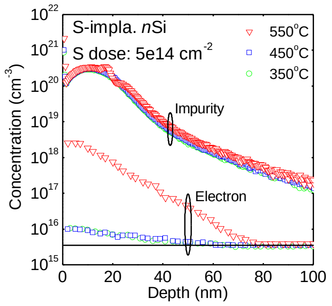

FIG. 1: Profiles of impurity and electron concentrations in S-implanted *n*Si(100).

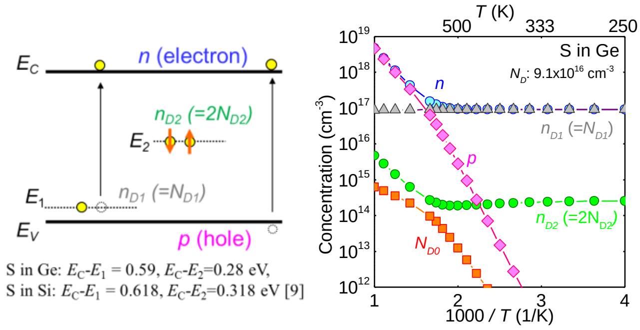

FIG. 2: (a) Band diagram for S in Si and in Ge, and (b) relationship between inverse temperature T and concentrations. n: electrons in E_C, p: holes in E_V, N_D: double donors, $n_{D1,2}$: electrons in donor level $E_{1,2}$.

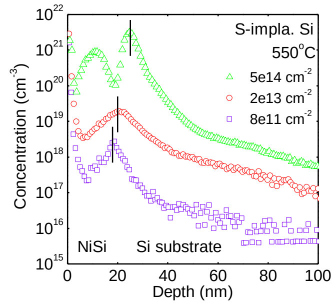

FIG. 4: Profiles of S-introduced NiSi/Si(100).

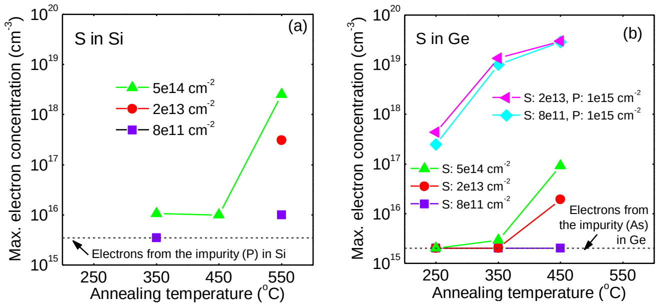

FIG. 3: Relationship between annealing temperature and maximum electron concentration in (a) Si and (b) Ge.

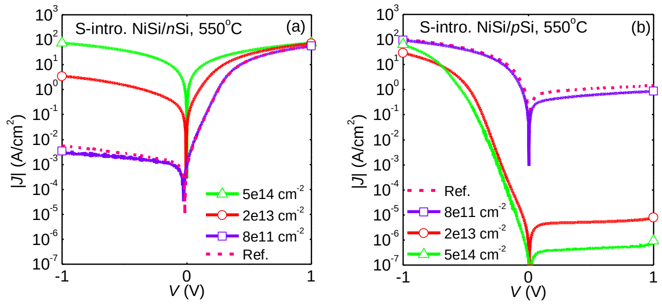

FIG. 5: *J-V* characteristics of S-introduced (a) NiSi/*n*Si and (b) NiSi/*p*Si.

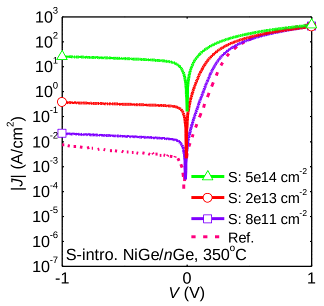

FIG. 6: *J-V* characteristics of S-introduced NiGe/*n*Ge.

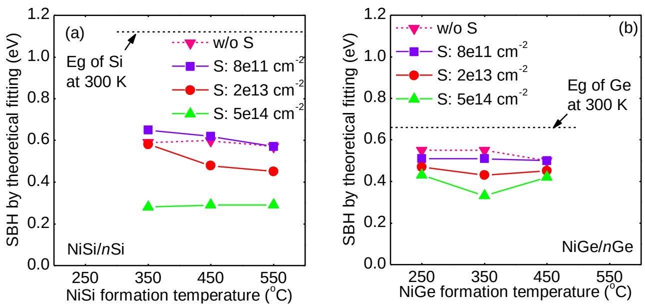

FIG. 7: Relationship between formation temperature and SBH for (a) NiSi/*n*Si and (b) NiGe/*n*Ge.

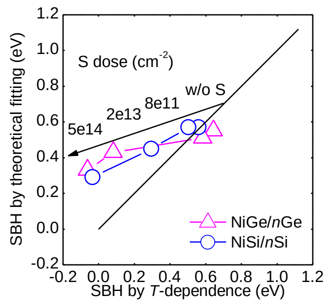

FIG. 8: Relationship between SBH values of NiGe/*n*Ge and NiSi/*n*Si estimated by two methods: theoretical fitting and temperature dependence.

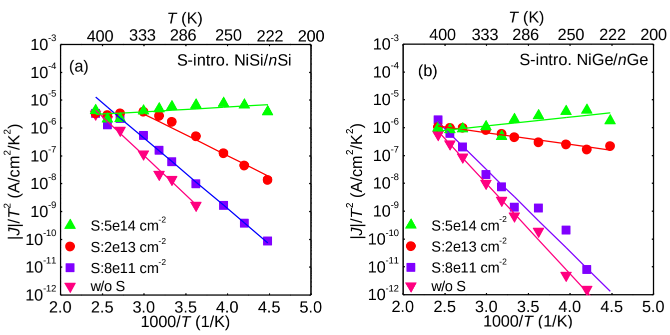

FIG. 9: Richardson plot for S-introduced (a) NiSi/*n*Si and (b) NiGe/*n*Ge.

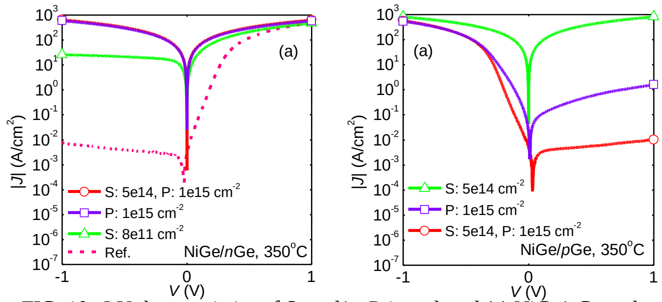

FIG. 10: *J-V* characteristics of S- and/or P-introduced (a) NiGe/*n*Ge and (b) NiGe/*p*Ge.